CAV2021
11th International Symposium on Cavitation
May 10-13, 2021, Daejon, Korea

A Numerical Study of Unsteady Hydrodynamic Characteristics on hydrofoils with leading edge protuberances: Cavitation Investigation with LES

Mohammad-Reza Pendar [1*], José Carlos Páscoa[1], Ehsan Roohi [2]

[1] Department of Electromechanical Engineering, University of Beira Interior, Portugal
[2] School of Aerospace Engineering, Xi'an Jiaotong University, China

Abstract: The impetus of this study is that it gives an in-depth insight into the unsteady hydrodynamic characteristics of the cavitating flow around a wavy leading edge (WLE) hydrofoils. Considered NACA 63_4-021 hydrofoil with WLE having a wavelength of 25% and an amplitude of 5% of the mean chord length and was compared to a straight-leading-edge (SLE) hydrofoil at cavitation numbers of σ=0.8 and a chord-based Reynolds number of 7.2×10^5. Here, detailed analyses of the fluid dynamic characteristics during the cloud cavitation evolution, i.e., vorticity stretching and dilatation; re-entrant jet; separation; spanwise flow and streamwise velocity fluctuation are investigated for a complete cycle of cloud cavitation around WLE and SLE hydrofoils. Our results indicate that the early development of the laminar separation bubble (LSBs) on the WLE hydrofoil suction side suppresses flow separation significantly. The results showed that the dynamics of the leading-edge vortex formation and flow separation were fundamentally different between the SLE and the WLE hydrofoil. The main difference between the WLE with SLE hydrofoil turbulent flow is the formation of counter-rotating streamwise vortices pairs. This research leads to an improvement in the knowledge that is required to investigate the performance of the hydrodynamic systems with WLE hydrofoil.

Keywords: Cavitation, Wavy leading edge (WLE) hydrofoil, Large eddy simulation (LES), Counter-rotation vortices

Introduction

Cavitation is a multi-phase incident that considerably affects hydrodynamic performance by causing lift reduction, erosion, vibration and noise. The perusal of the Humpback whale flippers for using as wavy leading edge (WLE) hydrofoils in various unsteady cavitating flows is instrumental. Fish and Battle [1] conducted research on the Humpback whale and found that the humpback whale is able to move and make sharp U-turns at high speeds. WLEs managed to restrict the flow separation at the wing tip area to the outboard region of the wing at a high angle of attack. Due to this managing, maximum lift coefficient increased and the stall angle could improve [1-4]. Recent studies have shown that although WLEs have an infinite span stall earlier than SLE, but the stall behavior is smoother. The performance of the foil may be higher for WLEs, especially the lift to drag ratio in the post-stall region [2, 5-6]. Higher values of pressure at the peaks and lower pressure at the troughs are shown in the study of pressure distributions in WLE hydrofoil. Due to the accelerated flow that is channeled between two adjoining peaks [3-4, 6], this low pressure is created. WLE geometries by reducing the unsteady fluctuations in the aerodynamic force [5-6] seems to be appropriate for applications that operate in highly disrupting flow conditions. Guerreiro and Sousa [7] showed that the sensitivity of performance to the Reynolds numbers for the WLE hydrofoils is lower than the SLE ones. Li et al. [8] compared a whalelike WLE modification numerically, along with a SLE hydrofoil. They researched the transient cloud cavitation structures and induced noise. Pendar et al. [9] employed the LES approach to study cavitation flow around a 3-D hydrofoil with a WLE with details.

* Corresponding Authors: m.reza.pendar@ubi.pt

Their results showed that flow separation is prevented by the early development of the laminar separation bubble on the wavy leading-edge hydrofoil's suction side. Custodio et al. [10] examined the cavitation around the hydrofoil with WLE experimentally and revealed that the cavity cloud with large amplitudes on the WLE hydrofoils was limited to the areas behind the troughs, while the entire span is covered by sheet cavity cloud in the SLE case. The current study numerically discusses the formation and evolution of the cavitation phenomenon over NACA 63$_4$-021 hydrofoils with WLE and SLE, using the LES method and the volume of fluid (VOF) approach.

Governing equations

In the current numerical study, the LES turbulence approach is considered to simulate the coupling between the Kunz cavitation mass transfer [11] and the unsteady Navier-Stokes equations. For tracking the contact surface between the cavity cloud and the water, a compressive volume of fluid (VOF) [12] procedure is adopted. To capture the details of the cavitating flow, the LES approach is quite appropriate and precisely depicts the flow characteristics [13-16].

Numerical strategy

Figure 1 represents a schematic display of the boundary conditions. As an inlet boundary, the inbounding flow velocity is imposed ($10 m/s$), and a specific values of the pressure is set at outlet to adjust the specified the cavitation number ($\sigma = (P - P_g)/0.5\rho U_\infty^2$). In all cases, the time step size was set at 1×10^{-8} to ensure that the Courant number is lower than 0.15. The chord-based Reynolds number is set at $Re = 7.2\times10^5$.

The structured meshes used over the computational domain is illustrated in Figure 2. Our purpose was to make isotropic and orthogonal grids with a small value of expansion factor. We performed our simulation with a total number of 15.2 million cells in the entire computational domain. As a validation purpose, the computed results for the lift and drag coefficients (figure 3 (a, b)) and vapor volume fraction (figure 3 (c, d)) are compared with the experimental data reported by Johari et al. [17] and Custodio et al. [10], respectively. An appropriate agreement between our numerical results and experimental data proves the suitability in predicting the considered flow.

Results and discussion

One complete cavity evolution cycle for the WLE and SLE hydrofoil is evaluated in Figure 4. The two cases' cavity cloud pattern is completely different, which causes change in the hydrodynamic force values, pressure, and vortical structure distribution. By comparing the isosurface of the zero time-averaged velocity that shows the boundary among the attached and separated flow, the exact difference between the SLE and WLE cases is the formation of the laminar separation bubble (LSB), i.e., the low-pressure zone, behind the troughs of the WLE hydrofoil (figure 5 (a)). It can be concluded in the SLE case, the separate flow region is larger than in the WLE case. The volume fractions contour with streamline in the SLE and WLE is compared in figure 5 (b). The existence of the tubercle causes an extended reverse flow with a large vortical structure.

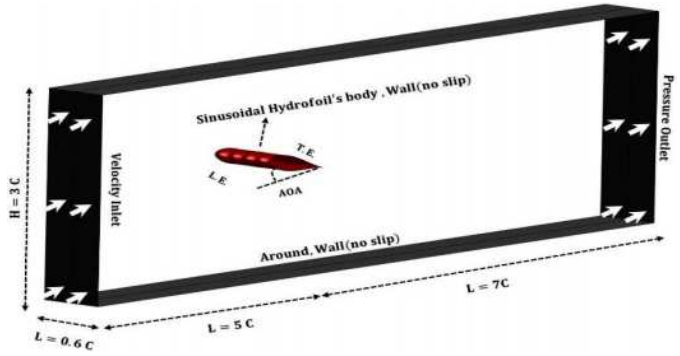

Figure 1. 3D view of the computational domain with boundary conditions.

* Corresponding Authors: m.reza.pendar@ubi.pt

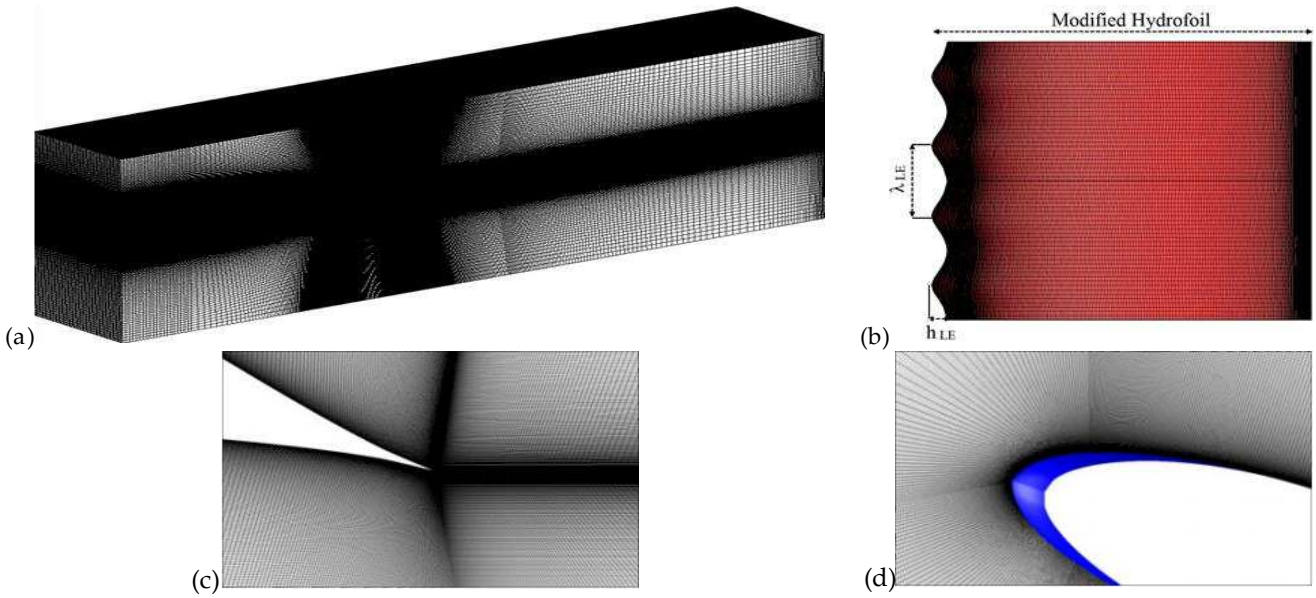

Figure 2. 3D structure grid generated around the NACA 63₄-021 hydrofoil.

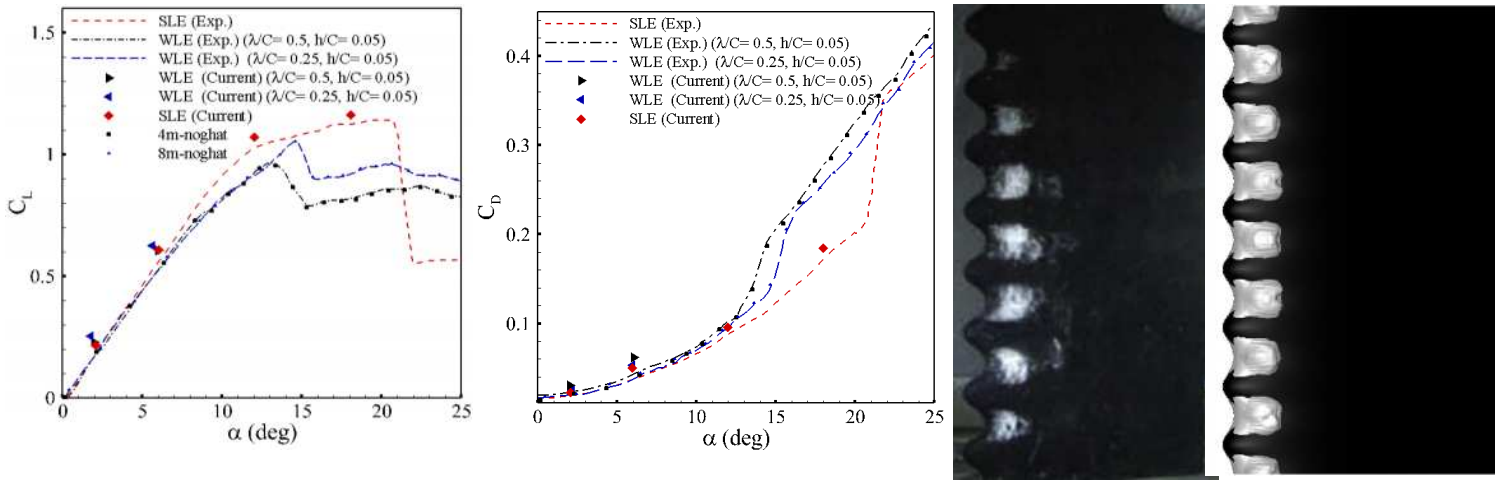

(a) lift coefficient (b) drag coefficient (c) Experimental (Custodio et al. [10]) (d) Current numerical result

Figure 3. Comparison of the (a, b) force coefficient and (c, d) vapor volume fraction with the experimental data ($\alpha = 18^{\circ}, \sigma = 4.23, h_{LE}/c_{ref} = 0.05, \lambda_{LE}/c_{ref} = 0.25, N_{peak} = 8$).

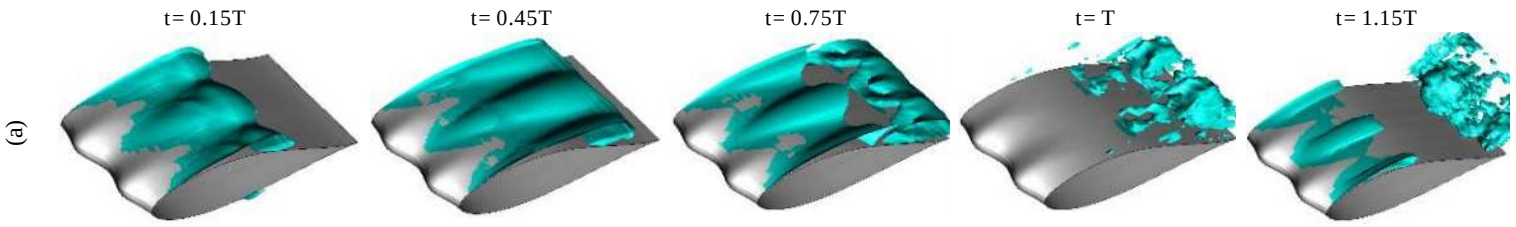

* Corresponding Authors: m.reza.pendar@ubi.pt

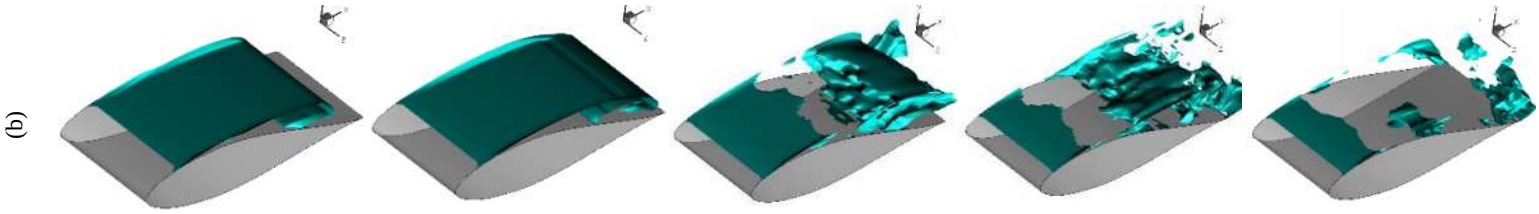

Figure 4. Iso-surfaces of volume fraction (α= 0.5) in one complete cavitation cycles (σ= 0.8) for (a) WLE and (b) SLE hydrofoil.

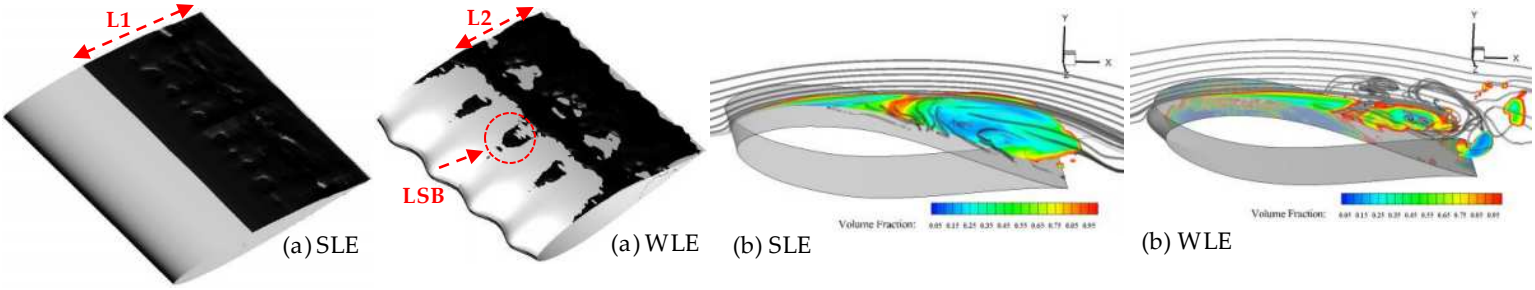

(a) SLE (a) WLE (b) SLE (b) WLE

Figure 5. The comparison of the isosurface of zero velocity (a), and the volume fraction with streamline (b) over the WLE and SLE hydrofoil (σ=0.8).

The re-entrant jet behavior over the SLE and various geometry of WLE hydrofoil with the presence of the cavity cloud region (α= 0.5) is compared in figure 6. The red and blue solid lines depict the boundary of the streamlines of the velocity and cavity cloud region, respectively. For the SLE case, the strong re-entrant jet is formed and attached to the body surface. But for the WLE cases, the re-entrant jet becomes dominant and causes cavity cloud breakdown and the most coherent shedding region. The smallest re-entrant jet region is formed by the WLE hydrofoil with the maximum amplitude (d).

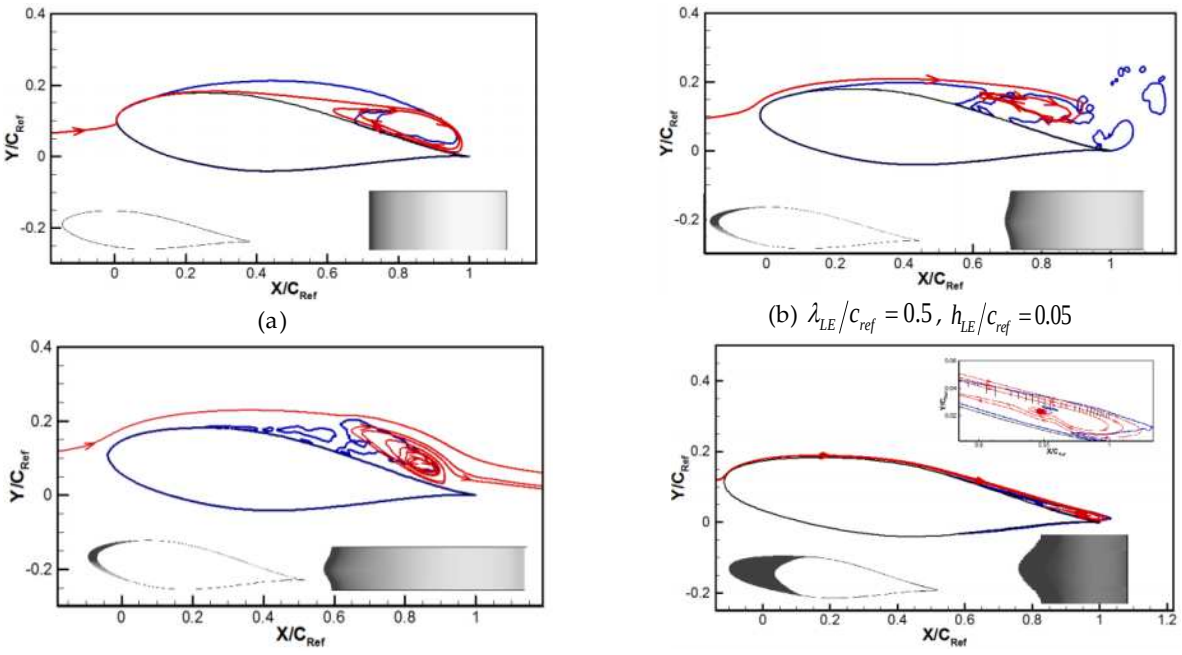

(a)

(b) $\lambda_{LE}/c_{ref} = 0.5$, $h_{LE}/c_{ref} = 0.05$

(c) $\lambda_{LE}/c_{ref} = 0.25$, $h_{LE}/c_{ref} = 0.05$

(d) $\lambda_{LE}/c_{ref} = 0.5$, $h_{LE}/c_{ref} = 0.25$

Figure 6. The visualization of the re-entrant jet pattern (displayed with streamlines mean-velocity) (red lines) and time-averaged volume fraction (blue lines) (σ =0.8).

* Corresponding Authors: m.reza.pendar@ubi.pt

Conclusions

Here, the cavitating flow characteristics over the WLE and SLE hydrofoil are compared by using the OpenFOAM framework. WLE significantly prevents flow separation due to the early development of the LSB, while the SLE causes entirely flow separation without reattachment. A detailed investigation of the cavity cloud dynamics through a complete cycle proves a different pattern with WLE. In the WLE cases, a spanwise flow over the suction side, a deflection towards the troughs, and a formation of a low-pressure zone behind the trough are observed.

Acknowledgments

This work was supported by Project " INTECH 4.0 –Novas Tecnologias para Fabricacao Inteligente", project grant no. POCI-01- 0247-FEDER-026653. The research was also partly supported by CMAST Center for Mechanical and Aerospace Science and Technology, research unit n° 151 from Fundacao para a Ciencia e Tecnologia (Portugal).

References

1. Fish, F. E. and Battle, J. M. Hydrodynamic design of the humpback whale flipper, J. Morphol. **1995**, 225 (1), 51–60.
2. Miklosovic, D. S., Murray, M. M., Howle, L. E. Experimental evaluation of sinusoidal leading edges, J. Aircraft **2007**, 44 (4), 1404–1408.
3. Pedro, H. T. C and Kobayashi, M. H. Numerical study of stall delay on humpback whale flippers. In 46th AIAA Aerospace Sciences Meeting and Exhibit **2008**.
4. Yoon, H.S., Hung, P.A., Jung, J.H., Kim, M.C. Effect of the wavy leading edge on hydrodynamic characteristics for flow around low aspect ratio wing, Int. J. Computers & Fluids **2011**, 49, 276–289.
5. Favier, J., Pinelli, A., Piomelli, U. Control of the separated flow around an airfoil using a wavy leading edge inspired by humpback whale flippers, C. R. Méc. **2012**, 340 (1–2), 107–114.
6. Skillen, A., Revell, A., Pinelli, A., Piomelli, U., Favier, J. Flow over a wing with leading-edge undulations, AIAA J. **2015**, 53 (2), 464–472.
7. Guerreiro, J. L. E. and Sousa, J. M. M. Low-Reynolds-number effects in passive stall control using sinusoidal leading edges, AIAA J. **2012** 50 (2), 461–469.
8. Li, Z., Qian, Z. and Ji, B. Transient cavitating flow structure and acoustic analysis of a hydrofoil with whale-like wavy leading edge. Applied Mathematical Modelling **2020**, 85, pp. 60-88.
9. Pendar, M.R., Esmaeilifar, E. and Roohi, E. LES study of unsteady cavitation characteristics of a 3-D hydrofoil with wavy leading edge. International Journal of Multiphase Flow **2020**, 132, p.103415.
10. Custodio, D., Henoch, C. and Johari, H. Cavitation on hydrofoils with leading edge protuberances. Ocean Engineering **2018**, 162, pp.196-208.
11. Kunz, R.F., Boger, D.A., Stinebring, D.R., Chyczewski, T.S., Lindau, J.W., Gibeling, H.J., Venkateswaran, S. and Govindan, T.R. A preconditioned Navier–Stokes method for two-phase flows with application to cavitation prediction. Computers & Fluids **2000**, 29(8), pp.849-875.
12. Hirt, C.W. and Nichols, B.D. Volume of fluid (VOF) method for the dynamics of free boundaries. Journal of computational physics **1981**, 39(1), pp.201-225.
13. Pendar, M.R. and Roohi, E. Detailed investigation of cavitation and supercavitation around different geometries using various turbulence and mass transfer models. In Journal of Physics: Conference Series **2015**, Vol. 656, No. 1, p. 012070.
14. Pendar, M.R. and Pascoa, J.C. Numerical Investigation of Electrostatic Spray Painting Transfer Processes for Vehicle Coating. SAE International Journal of Advances and Current Practices in Mobility **2020**, 2(2), pp.747-754.
15. Pendar, M.R. and Roohi, E. Investigation of cavitation around disk and conical cavitators using different sets of turbulence and cavitation models. In 4th International Conference on Advances in Mechanical Engineering-ICAME **2015**, May.
16. Pendar, M.R. and Páscoa, J.C. Atomization and spray characteristics around an ERBS using various operational models and conditions: numerical investigation. International Journal of Heat and Mass Transfer **2020**, 161, p.120243.
17. Johari, H., Henoch, C., Custodio, D., Levshin, L. Effects of leading-edge protuberances on airfoil performance, AIAA J. **2007**, 45, 2634–2642.

* Corresponding Authors: m.reza.pendar@ubi.pt